SURFACE ELEMENT METHOD BASED ON RING SOURCES FOR ACCURATE CALCULATIONS OF SHAPE FACTORS OF COMPLEX AXISYMMETRIC BODIES

M.M. Yovanovich[1] and C.S. Wang[2]
Department of Mechanical Engineering
University of Waterloo
Waterloo, Ontario, Canada

Abstract

A surface element method based on ring sources is developed to calculate shape factors of isothermal complex axisymmetric surfaces. A number of ring sources are used to replace the axisymmetric surface and then the temperatures of the surface are calculated simply by the temperature influence coefficients for ring sources. By selecting appropriate temperature points, whose temperatures represent the surface temperatures, the convergence process is accelerated. The appropriate temperature points in turn are located by some trial computing. Results are presented in tabular and graphical form for a range of aspect ratio for nine types of isothermal bodies (92 cases): the sphere, oblate and prolate spheroids, two-tangent spheres, right-circular cylinder, single cone, double cone, spherical caps (including hemisphere) and the square toroid. All computations are completed on a microcomputer (386PC) and the numerical results are in excellent agreement with existing exact solutions.

Nomenclature

A	=	surface area of the body
AR	=	aspect ratio of oblate and prolate spheroids
a	=	radius of a ring source
D	=	diameter of the largest cross-section for the oblate and prolate spheroids, single cone and double cone, and diameter of cylinder cross-section
D_1, D_2	=	the two diameters of the two-tangent spheres
e	=	the eccentricity of the prolate spheroid
G_{ij}	=	influence coefficient between temperature point i and ring source j
H	=	heights of the oblate and prolate spheroids
$K(\kappa)$	=	complete elliptic integral of the first kind
k	=	thermal conductivity of the extensive medium
L	=	length of the cylinder
$\mathcal{L}$	=	characteristic length of the body
N	=	number of ring sources
n	=	outward body normal
$Nu_{\mathcal{L}}$	=	Nusselt number $[Nu_{\mathcal{L}} = h\mathcal{L}/k]$
P	=	position ratio related to the position of temperature point
$P_{n-1/2}(\xi)$	=	toroid function
Q	=	total heat flow rate
$Q_{n-1/2}(\xi)$	=	toroid function
Q_j	=	source strength of ring j
Ra	=	Rayleigh number $[Gr_{\mathcal{L}}Pr = g\beta(T_0 - T_\infty)\mathcal{L}^3/\nu\alpha]$
r	=	radial coordinate
$r1, r2$	=	the two radii of the two-tangent spheres
S	=	shape factor
$S^*_{\mathcal{L}}$	=	dimensionless shape factor $[S\mathcal{L}/A]$
$S^*_{\sqrt{A}}$	=	dimensionless shape factor with $\mathcal{L} = \sqrt{A}$
T_i	=	temperature rise at point i
T_{il}	=	temperature rise at point i due to local ring source
T_{io}	=	temperature rise at point i due to the other ring sources
T_0	=	uniform body temperature
T_∞	=	medium temperature remote from the body
u	=	aspect ratio of the oblate and prolate spheroids
z	=	axial coordinate
γ	=	Euler's constant
ϕ	=	dimensionless temperature
κ	=	modulus of elliptic integrals
ξ	=	toroid diameter ratio
ψ	=	PolyGamma function

Motivation For The Study

Steady-state heat transfer from isothermal bodies of complex shape into a medium of thermal conductivity k is currently of some interest to thermal analysts who are concerned with developing models of natural convection heat transfer from a single body [1–16]. As the Rayleigh number decreases approaching very small values, say $Ra < 1$, the Nusselt number approaches the diffusive asymptote which corresponds to pure conduction from the body into the full space surrounding it [5,16].

[1]Professor of Mechanical Engineering, Fellow AIAA
[2]Graduate Research Assistant

This problem is encountered in many industrial applications including heat transfer from microelectronics components.

The ability to calculate quickly and accurately the shape factor of bodies having complex geometries is one of the more difficult conduction problems faced by the thermal analysts. Frequently numerical solutions based on the finite difference or finite element methods [4, 5] which require discretization of the full space surrounding the body are used to obtain the unknown shape factor. Both methods are time consuming and expensive. An alternate method requiring less time to set up, which is more accurate and far less expensive would be well-received by the community.

In addition, in previous papers on the surface element method several planar contact surfaces on a half space have been considered; the contact area temperatures due to the uniform heat flux can be obtained and hence the analytical constriction resistances and the shape factors are available [17, 18].

For Dirichlet contacts, a formulation has been presented for the numerical prediction of the thermal constriction resistance due to arbitrary planar contacts located on a half-space [15].

But the surface element method applied to a contact of curved surface has not been reported.

In the present paper arbitrary axisymmetric isothermal surfaces surrounded by a full space are considered, and a new approach to the problem is presented.

Problem Statement

An arbitrary axisymmetric body, for example a right circular cylinder, is situated in a full space of thermal conductivity k (Figure 1).

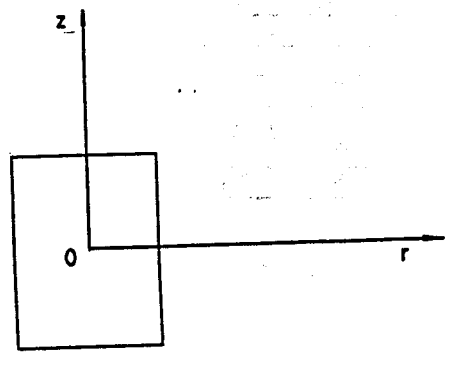

Figure 1: Right-circular cylinder surface in a full space.

Heat enters the full space through the entire surface of the body and flows steadily through the conducting medium to infinity. Over the entire body surface, the temperature is uniform (T_0). The temperature within the full space tends towards a uniform temperature (T_∞) at points far from the isothermal body surface. For convenience, this temperature will be taken to be zero.

The problem is formulated in circular cylinder coordinates (r, z). The dimensionless temperature $\phi(r,z) = (T(r,z) - T_\infty)/(T_0 - T_\infty)$ is the solution of the Laplace equation:

$$\frac{\partial^2\phi}{\partial r^2} + \frac{1}{r}\frac{\partial\phi}{\partial r} + \frac{\partial^2\phi}{\partial z^2} = 0 \quad 0 \le r < \infty, \quad -\infty < z < +\infty \tag{1}$$

The solution $\phi(r,z)$ must satisfy the symmetry boundary condition along the axis:

$$\frac{\partial\phi}{\partial r} = 0, \qquad r = 0, \qquad -\infty < z < +\infty$$

as well as the regular condition $\phi(r,z) \to 0$ at remote points, $\sqrt{r^2+z^2} \to \infty$.

The parameter of interest in this study is the thermal shape factor S defined by

$$Q = k\ S\ (T_0 - T_\infty) \tag{2}$$

where Q is the total heat transfer rate from the total surface A of the body:

$$Q = \iint_A -k(T_0 - T_\infty)\frac{\partial\phi}{\partial n}\, dA$$

From the above definitions we have for the shape factor per unit area of the body:

$$\frac{S}{A} = \frac{1}{A}\iint_A -\frac{\partial\phi}{\partial n}\, dA$$

The dimensionless shape factor is defined as

$$S^*_{\mathcal{L}} = \frac{S}{A}\,\mathcal{L} = \frac{\mathcal{L}}{A}\iint_A -\frac{\partial\phi}{\partial n}\, dA \tag{3}$$

where n is the outward-directed normal to the surface of the body.

In this paper it will be shown that the dimensionless shape factor defined above is a weak function of the body shape [7] with respect to the characteristic body length $\mathcal{L} = \sqrt{A}$. The diffusive Nusselt number defined as $Nu = Q\mathcal{L}/(Ak[T_0 - T_\infty])$ and the shape factor $S^*_{\mathcal{L}}$ are related; and, from the above definitions, we have $S^*_{\mathcal{L}} = Nu_{\mathcal{L}}$.

In order to determine the shape factor, we need to obtain the total heat flow rate Q.

Description of The Method

In a full space the temperature rise at an arbitrary point (r,z) due to a thermal point source of strength dQ is [17, 18]:

$$T(r,z) = \frac{1}{4\pi k}\frac{dQ}{r}$$

where r is the distance from the thermal point source dQ to the arbitrary point (r,z).

By superposition the temperature rise at the arbitrary point due to a surface source is

$$T(r,z) = \frac{1}{4\pi k}\iint_A \frac{q}{r}\,dA \tag{4}$$

where A is an arbitrary surface source, for example, a right-circular cylinder surface, and $qdA = dQ$.

For isothermal contact problems, as described in [15], the contact surface is subdivided into N subregions and Eq. (4) can be written as

$$T(r,z) = \frac{1}{4\pi k}\sum_{j=1}^{N}\iint_{A_j} \frac{q}{r}\,dA_j \tag{5}$$

where A_j is subregion j.

If the contact surface is planar, the integral in Eq. (5) can be integrated and numerical procedures for the problem have been presented [15].

But, in the case of complex axisymmetric surfaces, the integral in Eq. (5) is difficult or impossible to integrate, even though the heat flux q is constant for each subregion.

So we assume that the source strength of each subregion is concentrated at its central ring, i.e. each subregion source is replaced by a ring source of the same strength. In Figure 3, for example, the cylinder surface is subdivided into 8 subregions and they are replaced by 8 ring sources on the surface: two on the top surface, another two on the bottom surface and the other four on the lateral surface. Thus the integral in Eq. (5) becomes the ring source integral and the equation derived for the ring source can be used directly [17].

For a uniform circular ring source with origin of coordinates at its center, with reference to Figure 2, the equation below can be used to calculate the temperature rise at an arbitrary field point (r,z) [17]:

$$T(r,z) = \frac{Q}{4\pi k}\frac{2}{\pi}\frac{1}{\sqrt{(r+a)^2+z^2}}K(\kappa) \tag{6}$$

where $K(\kappa)$ is the complete elliptic integral of first kind of modulus κ, a is the radius of the ring and

$$\kappa^2 = \frac{4ra}{(r+a)^2+z^2}$$

In Figure 3 for the temperature rise at point i due to ring source j, Eq. (6) can be conveniently expressed in the following manner:

$$T_{ij} = G_{ij}\,Q_j \tag{7}$$

where

$$G_{ij} = \frac{1}{4\pi k}\frac{2}{\pi}\frac{K(\kappa_{ij})}{\sqrt{(r_i+a_j)^2+z_{ij}^2}}$$

Q_j is the source strength of ring j and

$$\kappa_{ij}^2 = \frac{4r_i a_j}{(r_i+a_j)^2+z_{ij}^2}$$

where r_i is the distance from the temperature point i to the z-axis, a_j is the radius of ring j, z_{ij} is the distance from point i to the plane of ring j.

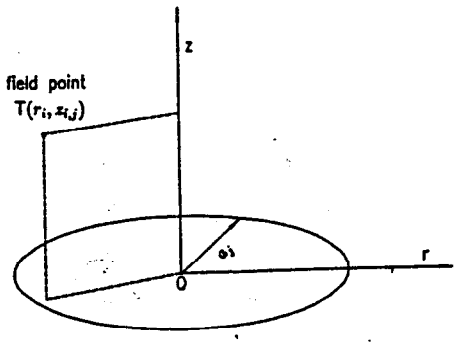

Figure 2: Uniform circular ring source.

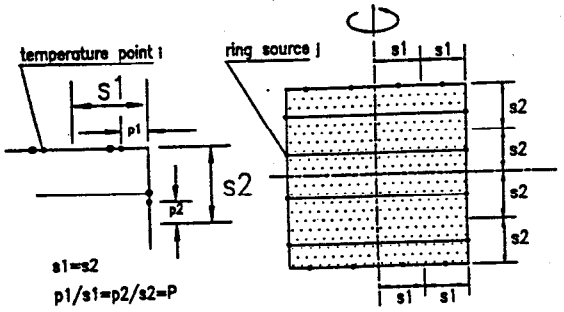

Figure 3: Cylinder surface with ring sources.

By means of Eq. (7), Eq. (5) becomes

$$T_i = \sum_{j=1}^{N} G_{ij}\,Q_j \tag{8}$$

where T_i represents the total temperature rise at point i.

Now, on each subregion select a point near the local ring source as the temperature point whose temperature represents that of the corresponding subregion. Therefore in Figure 3, there are 8 ring sources and 8 temperature points.

The successive application of Eq. (8) to each selected temperature point then results in the system of algebraic equations:

$$[G_{ij}]\{Q_j\} = \{T_i\} \tag{9}$$

where $i = 1,2,3,\cdots N$; $j = 1,2,3,\cdots N$.

For the isothermal surface, T_i is prescribed, the solution of Eqs. (9) yields the distribution of the ring source strengths $\{Q_j\}$.

The total heat flow rate Q is equal to the sum of the N ring source strengths $\{Q\}$:

$$Q = \sum_{j=1}^{N} Q_j$$

Because $T_i = T_0 =$ Constant and $T_\infty = 0$ then the shape factor is obtained:

$$S = \frac{Q}{k(T_0 - T_\infty)} = \frac{Q}{k\,T_0} \tag{10}$$

and nondimensionalized with $\mathcal{L} = \sqrt{A}$:

$$S^*_{\sqrt{A}} = \frac{S}{\sqrt{A}} = \frac{1}{k\,T_0\sqrt{A}} \sum_{j=1}^{N} Q_j \tag{11}$$

Convergence Study

Physically, as N goes to infinity the ring sources as a whole will approach a continuous surface source, and hence the temperatures at the selected points will approach the exact values of the considered surface. But generally they converge very slowly, if the temperature points are allocated arbitrarily. However, by selecting appropriate temperature points, it is possible to accelerate the convergence process.

In order to give a clear explanation, consider the inverse problem first. With reference to Figure 3, assume the ring source strengths have been known, then the temperatures at the selected points can be calculated by Eq. (8). Now we rewrite Eq. (8) in the following form:

$$T_i = G_{ii}\,Q_i + \sum_{j=1, j\neq i}^{N} G_{ij}\,Q_j \tag{12}$$

or simply

$$T_i = T_{il} + T_{io} \tag{13}$$

where T_{il} is the temperature rise only due to the local ring source and T_{io} is that due to the other ring sources. As N increases the variations of T_{il}, T_{io} and T_i are illustrated qualitatively in Figure 4.

With reference to Figure 3, we define the position ratio P as below:

$$P = \frac{p_i}{s_i}$$

where s_i is the width of subregion i and p_i is the distance from the temperature point i to the edge of the corresponding subregion. In Figure 3 s_i is equal to $s1$ and p_i is equal to $p1$ for the subregions on the top or the bottom surface, while they are equal to $s2$ and $p2$ respectively for those on the lateral surface. In our case we make $P = p1/s1 = p2/s2$.

For different values of P, the variations of T_{il} and T_{io} are shown in Figure 5.

In Figure 4 and Figure 5 it can be seen that as N increases, T_{io} increases while T_{il} decreases; in addition, for different values of P, T_{io} does not vary much but T_{il} varies significantly. Therefore, by changing the location of the temperature points, i.e. by changing the values of P, we can adjust the magnitude of T_{il} and thereby adjust T_i and its convergence characteristic.

By means of trial computing, one can find the appropriate value of P, at which T_i approaches its asymptotic value very quickly.

As shown qualitatively in Figure 6, when $P = 0.4$, i.e. the temperature point is close to the local ring source, T_i converges slowly from above because the rate of decrease of T_{il} is dominant, with reference to Eq. (13) and Figure 5.

When $P = 0.2$, i.e. the temperature point is at a relatively large distance from the local ring source, T_i converges slowly from below because the rate of increase of T_{io} is dominant instead.

If $P = 0.333$, T_i converges very quickly. At the be-

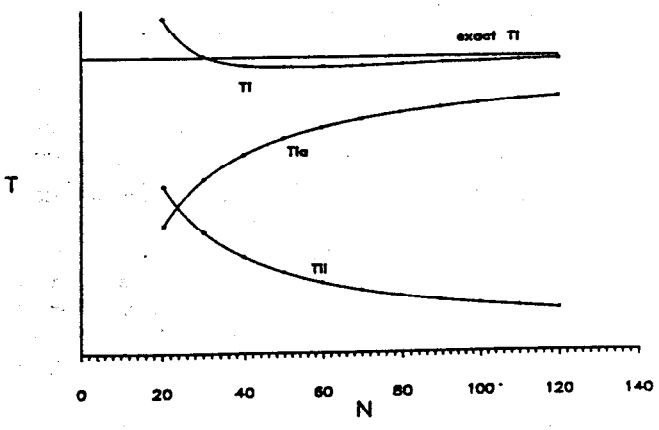

Figure 4: Variations of T_{il}, T_{io} and T_i with N.

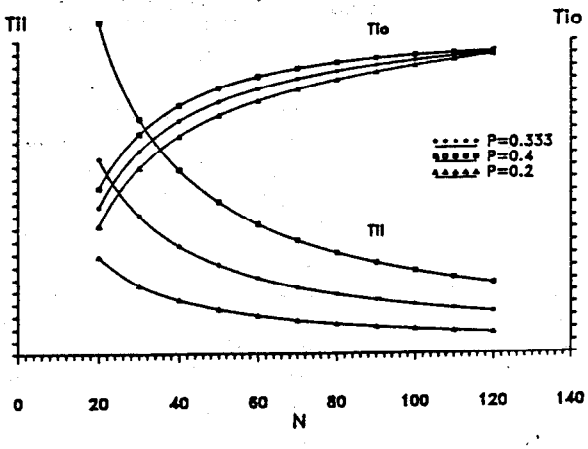

Figure 5: Variations of T_{il} and T_{io} with N and P.

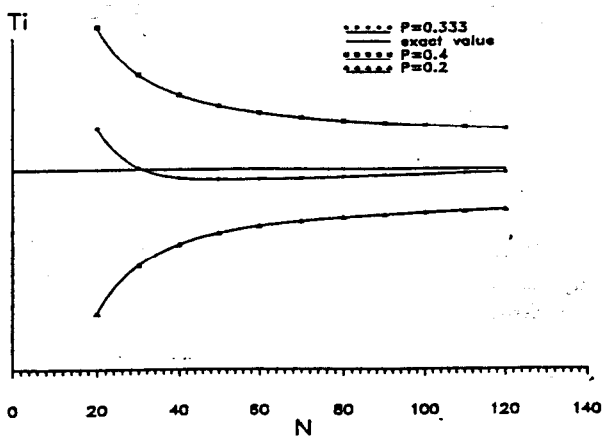

Figure 6: Variations of T_i with N for different P.

ginning ($N < 60$), T_i decreases. But beyond some point ($N > 60$), T_i increases instead. At this value of P, the rate of decrease of T_{il} and the rate of increase of T_{io} with N are approximately equal to each other. Therefore, we can determine the appropriate value of P in the following manner:

While repeating the computation, for a selected value of P, increase N step by step and observe the sign of $\Delta T_i = T_i(N_{k+1}) - T_i(N_k)$, where N_k is the number of the ring sources for kth computation and $N_{k+1} > N_k$, for example $N_{k+1} - N_k = 10$ with reference to Figure 6. If the value P is appropriate, the sign of ΔT_i will change at a certain value of N, for example $N = 60$ in Figure 6 for $P = 0.333$. It indicates that at this value of P, the rate of decrease of T_{il} and the rate of increase of T_{io} with N are approximately equal to each other, and hence T_i converges quickly.

If the value of P is not appropriate, the sign of ΔT_i will remain the same while our repeating computation and the absolute value of ΔT_i will be relatively large. In this situation, change the value of P according to the sign and the absolute value of ΔT_i and repeat the computation until the appropriate value of P is found.

Now return to the original problem. In the isothermal problem, $\{T_i\}$ is fixed and we solve Eqs. (9) for $\{Q_j\}$. The effect of the location of the temperature point(the value of P) on Q_j is similar to the effect of the value of P on the T_i. We find the appropriate value of P as described above, and therefore, the dimensionless shape factor, Eq. (11), can be computed accurately.

The following Figure 7 and Figure 8 are drawn from our results given later. They show the convergence characteristic of the present results. Figure 7 is the convergence curve of the dimensionless shape factor $S^*_{\sqrt{A}}$ for sphere, it approaches the exact value very quickly as N growing large. In the case, we take $P = 0.3332$. At beginning, the value of $S^*_{\sqrt{A}}$ increases, but beyond the point($N = 70$), the value decreases instead.

Figure 8 is the convergence curve for a solid cone with P=0.3. It can be seen that the value of $S^*_{\sqrt{A}}$ for cone also approaches the assumed asymptotic value quickly, when N growing large.

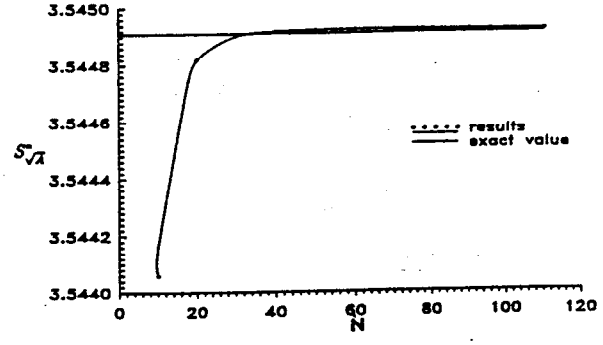

Figure 7: Variations of shape factor of sphere with N, for $P = 0.3332$.

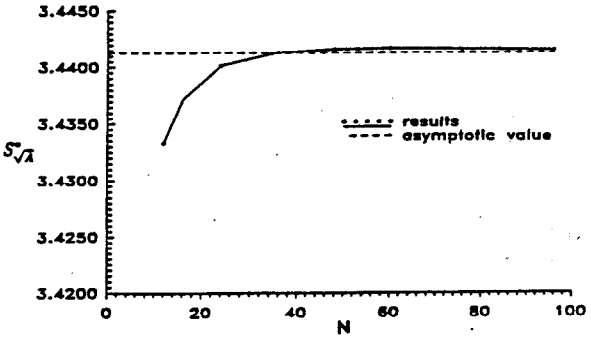

Figure 8: Variations of shape factor of cone with N, for $H/D = 1.0$, $P = 0.3$.

Some Results and Their Comparison with Exact Values

In the following, five sets of results obtained by the present method for the sphere, oblate and prolate spheroids, two-tangent spheres and the right-circular cylinder show very good agreement with exact solutions or other existing solutions.

For convenience the analytic dimensionless shape factor $S^*_{\sqrt{A}}$ for the following geometries: oblate and prolate spheroids, the two-tangent spheres, the bisphere, the circular toroid and the right-circular cylinder are given below with reference to Figure 9 and Figure 11.

Oblate Spheroids

$$S^*_{\sqrt{A}} = \sqrt{\frac{\pi}{2}}\, 4e \left\{ \left[1 + \frac{u^2}{e} \frac{1}{2} \ln\left(\frac{1+e}{1-e}\right) \right]^{\frac{1}{2}} \cos^{-1} u \right\}^{-1}$$

Prolate Spheroids

$$S^*_{\sqrt{A}} = \sqrt{\frac{\pi}{2}}\, 4e \left\{ \left[u^2 + \frac{u}{e} \sin^{-1} e \right]^{\frac{1}{2}} \frac{1}{2} \ln\left(\frac{1+e}{1-e}\right) \right\}^{-1}$$

where $u = c/b$ and $e = \sqrt{1-u^2}$, which is called the eccentricity. The aspect ratio is $AR = u$ for the oblate spheroids and $AR = 1/u$ for the prolate spheroids.

If the aspect ratio of the prolate spheroid is greater than 8, the solution approaches the asymptote:

$$S^*_{\sqrt{A}} = \frac{4\sqrt{AR}}{\ln(2AR)}$$

Two-Tangent Spheres

$$S^*_{\sqrt{A}} = -\frac{2\sqrt{\pi}\,r1\,r2}{(r1+r2)\sqrt{r1^2+r2^2}} \left\{2\gamma + \psi\left(\frac{r1}{r1+r2}\right) + \psi\left(\frac{r2}{r1+r2}\right)\right\}$$

where $r1 = D_1/2$ and $r2 = D_2/2$ are the sphere radii respectively, and $2\gamma = 1.15443$.

The PolyGamma function ψ and its properties are given in Abramowitz and Stegun.

If $r1 = r2$, the two-tangent spheres solution reduces to the bisphere solution:

$$S^*_{\sqrt{A}} = 3.475$$

If $r1 >> r2$, the two-tangent spheres solution goes to the single sphere solution:

$$S^*_{\sqrt{A}} = 3.5449$$

Circular Toroid

$$S^*_{\sqrt{A}} = \frac{4}{\pi}\sqrt{\xi - 1/\xi}\left\{\frac{Q_{-1/2}(\xi)}{P_{-1/2}(\xi)} + 2\sum_{n=1}^{\infty}\frac{Q_{n-1/2}(\xi)}{P_{n-1/2}(\xi)}\right\}$$

with $\xi = D/d > 1$. The functions which appear in the solution are Toroidal (or ring) functions whose properties are given in Abramowitz and Stegun [19].

The special functions appearing in the above solutions can be accurately computed using *Mathematica* [20].

The solution for the toroid for $D/d > 5$ approaches the asymptote:

$$S^*_{\sqrt{A}} = \frac{2\pi\sqrt{D/d}}{\ln(8D/d)}$$

Circular Cylinder

The correlation equation of Smythe [13,14] for the right-circular cylinder has been nondimensionalized with $\mathcal{L} = \sqrt{A}$:

$$S^*_{\sqrt{A}} = \frac{3.1915 + 2.7726\,(L/D)^{0.76}}{\sqrt{1+2\,(L/D)}}$$

where L/D is the aspect ratio and it is limited to the range $0 \le L/D \le 8$.

In Table 1 the excellent result is obtained with 20 ring sources. If N is larger, the result is even more accurate with reference to Figure 7.

Table 1: Result for isothermal sphere.

Number of rings	Present result	Exact result	Error %
20	3.5448	3.5449	-0.003

The numerical results for oblate and prolate spheroids for a large range of aspect ratio, $(0.10 \le AR \le 20)$ based on 10 ring sources are presented in Table 2, and they are seen to be in very good agreement with the exact solutions given above. The large percent difference observed for $AR \ge 8$ can be reduced significantly by increasing the number of rings.

Table 2: Comparison of present method with exact solution for oblate and prolate spheroids for $0 \le AR \le 20$.

Geometry	AR (H/D)	Number of rings	Present results	Exact solution	Percent difference
Oblate	0.10	10	3.337	3.344	-0.209
"	0.30	10	3.480	3.482	-0.057
"	0.50	10	3.524	3.529	-0.142
"	0.70	10	3.537	3.542	-0.141
"	0.90	10	3.538	3.545	-0.197
"	0.999	10	3.541	3.545	-0.113
Prolate	1.20	10	3.548	3.545	+0.085
"	1.40	10	3.549	3.547	+0.056
"	1.60	10	3.553	3.552	+0.028
"	1.80	10	3.560	3.558	+0.056
"	2.00	10	3.568	3.566	+0.056
"	4.00	10	3.701	3.706	-0.135
"	8.00	10	4.022	4.040	-0.446
"	10.00	10	4.172	4.195	-0.548
"	20.00	10	4.812	4.841	-0.743

As to two-tangent spheres, the computation based on about 10 ring sources gives very good results for any radius ratio $(r1/r2)$ as shown in Table 3.

Table 3: Comparison of present method with exact solution for two-tangent spheres for $0 < r1/r2 \le 1$.

r1/r2	Number of rings	Present results	Exact solution	Percent difference
1.000	10	3.474	3.475	-0.02
0.800	9	3.475	3.476	-0.03
0.600	9	3.477	3.479	-0.06
0.400	9	3.483	3.490	-0.2
0.200	10	3.526	3.516	+0.3
0.100	11	3.535	3.534	+0.03
0.001	11	3.545	3.545	0.0

The present numerical results for the right-circular cylinder for $(0.1 \le AR \le 8)$ based on $12-20$ rings are given in Table 4. The results are in very good agreement with the Smythe correlation which is based on analytic methods.

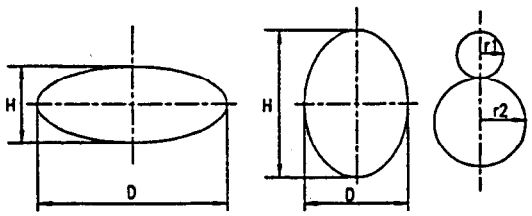

Figure 9: Oblate, prolate and two-tangent spheres.

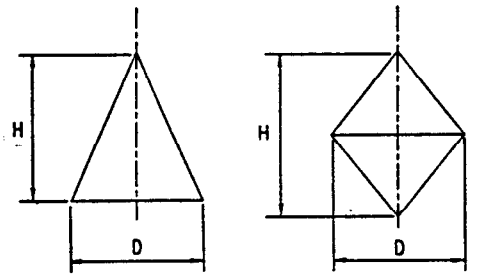

Figure 10: Single and double cone.

Table 4: Comparison of present method with existing solution for right-circular cylinder for $0.1 \leq H/D \leq 8.0$.

AR (H/D)	Number of rings	Present results	Smythe correlation	Percent difference
0.1	12	3.3469	3.3533	-0.191
0.2	12	3.3880	3.3871	+0.027
0.4	14	3.4176	3.4089	+0.256
0.6	16	3.4328	3.4196	+0.384
0.8	18	3.4451	3.4306	+0.420
1.0	20	3.4578	3.4435	+0.415
2.0	18	3.5392	3.5272	+0.340
4.0	20	3.7208	3.7144	+0.171
6.0	14	3.9000	3.8867	+0.343
8.0	18	4.0563	4.0402	+0.398

Additional Numerical Results

In the following, we give results for the isothermal single cone, double cone, spherical cap, and the square toroid, whose exact solutions are presently unknown.

In order to give accurate results, a large number of ring sources was used for the solid cone and double cone shown in Figure 10. The numerical results for the single cone with $N = 100$ in Table 5, and the numerical results for the double cone with $N = 60$ in Table 6 are presented. It is believed that at least 3 digits of the result are correct and the result should be slightly greater than the unknown exact solution with reference to Figure 8 for the single cone. It is expected that the accuracy of the results for double cone is similar to that of the single cone.

Table 5: Results for isothermal solid cone ($N = 100$).

Aspect ratio (H/D)	Present results	Aspect ratio (H/D)	Present results
8.0	4.3852	0.6	3.3781
4.0	3.8972	0.4	3.3412
2.0	3.5983	0.2	3.2861
1.0	3.4413	0.1	3.2447
0.8	3.4096	0.001	3.1908

Table 6: Results for isothermal double cone ($N = 60$).

Aspect ratio (H/D)	Results	Aspect ratio (H/D)	Results
0.001	3.1951	0.8	3.4503
0.1	3.2521	0.9	3.4613
0.2	3.3003	1.0	3.4711
0.3	3.3423	2.0	3.5595
0.4	3.3755	4.0	3.7842
0.5	3.4008	6.0	4.0150
0.6	3.4205	8.0	4.2297
0.7	3.4371	10.0	4.4248

Table 7 gives the results for the solid spherical cap including the hemisphere (ω=90). At the two limits ($\omega \rightarrow 0$ and $\omega \rightarrow 180$), the results approach the exact values for the disk and the sphere, i.e. $S^*_{\sqrt{A}} = 3.1915$ for the disk and $S^*_{\sqrt{A}} = 3.5449$ for the sphere.

Table 7: Results for isothermal solid spherical cap ($N = 60$).

ω(degree)	Results	ω(degree)	Results
0.5	3.1956	100	3.4800
10	3.2364	110	3.4977
20	3.2737	120	3.5129
30	3.3076	130	3.5254
40	3.3387	140	3.5347
50	3.3667	150	3.5406
60	3.3926	160	3.5437
70	3.4171	170	3.5446
80	3.4397	179.5	3.5449
90	3.4606		

Table 8 gives the results for the square toroid which are compared with the exact solution of the corresponding circular toroid, for which $D = 2(r_0 - 0.5s), \pi d = 4s$ with reference to Figure 11, i.e. the two major diameters are set equal and the two perimeters of the two cross-sections are set equal. We observe that as $s/r_0 \rightarrow 0$, the numerical results for the square toroid approach the analytic solution of the equivalent circular toroid.

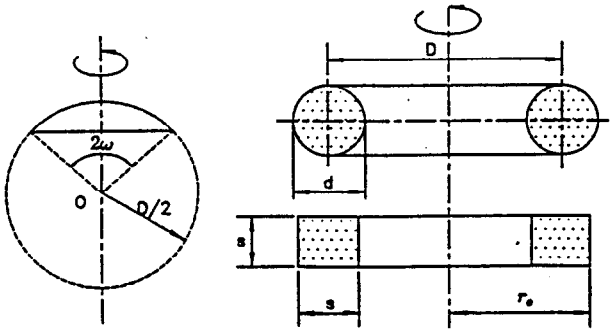

Figure 11: Spherical cap, square and circular toroids.

Table 8: Results for isothermal square toroid ($N = 96$).

s/r_0	Present results for square toroid	Exact solution for corresponding circular toroid
0.9999	3.4185	
0.9	3.3451	
0.8	3.3015	3.440
0.7	3.2885	3.411
0.6	3.3098	3.425
0.5	3.3738	3.479
0.4	3.4964	3.583
0.3	3.7116	3.797
0.2	4.1064	4.188
0.1	5.0120	5.075
0.05	6.2414	6.321
0.01	10.9011	11.015
0.001	26.1700	26.378
0.0001	66.6423	67.068

Summary and Conclusions

The surface element method based on ring sources has been presented to obtain accurate numerical values of the dimensionless shape factor for an arbitrary, isothermal axisymmetric surface. The proposed method does not require much memory space and computing time, and hence is easy to implement on personal computers.

The convergence process is accelerated by a novel location optimum of temperature points.

Extremely accurate results with errors $< 1\,\%$ are presented and even more accurate results can be obtained easily by increasing the number of the rings, if necessary.

It is shown that the dimensionless shape factor is a weak function of the body shape [7, 16] with respect to the characteristic body length $\mathcal{L} = \sqrt{A}$.

Numerical results are presented in tabular form for nine types of isothermal bodies: the sphere, oblate and prolate spheroids, two-tangent spheres, right-circular cylinder, single cone, double cone, spherical caps(including hemisphere) and the square toroid for a range of aspect ratio.

The proposed surface element method based on ring source has the potential to be applied to multiple axisymmetric bodies or single axisymmetric bodies with multiply-connected surfaces.

Acknowledgment

The authors acknowledge the financial support of the Natural Sciences and Engineering Research Council of Canada under operating grant A7455 for Dr. Yovanovich.

References

1. Raithby, G. D. and Hollands, K. G. T., "A General Method of Obtaining Approximate Solutions to Laminar and Turbulent Free Convection Problems," *Advances in Heat Transfer*, Vol. 11, Academic Press, 1975, pp. 265-315.

2. Powe, R. E., Warrington, R. O., and Scalan, J. S., "Natural Convection Heat Transfer Between Bodies and Their Spherical Enclosure," ASME Publication HTD Vol. 8, 19th National Heat Transfer Conference, Orlando, Fla., July 1980, pp. 79-87.

3. Warrington, R. O. and Powe, R. E., "Natural Convection Between Bodies and Their Enclosures," ASME Publication HTD Vol. 16, 20th National Heat Transfer Conference, Milwaukee, Wis., 1981, pp. 111-125.

4. Warrington, R. O., Powe, R. E. and Mussulman, R. L., "Steady Conduction in Three-Dimensional Shells," ASME Journal of Heat Transfer, Vol. 104, May 1982, pp. 393-394.

5. Hassani, A. V. and Hollands, K. G. T., "Conduction Shape Factor for a Region of Uniform Thickness Surrounding a Three-Dimensional Body of Arbitrary Shape," ASME Journal of Heat Transfer, Vol. 112, May 1990, pp. 492-495.

6. Greenspan, D., "Resolution of Classical Capacity Problem by Means of a Digital Computer," *Canadian J. of Physics*, Vol. 44, 1966, pp. 2605-2614.

7. Chow, Y. L. and Yovanovich, M. M., "The Shape Factor of the Capacitance of a Conductor," *Journal of Applied Mechanics*, Vol. 53, No. 12, 1982, pp. 8470-8475.

8. Hahne, E. and Grigull, U., "Formfaktor und Formwiderstand der Stationaren Mehrdimensionalen Warmeleitung," *Int. J. Heat Mass Transfer*, Vol. 18, 1975, pp. 751-767.

9. Hahne, E. and Grigull, U., "A Shape Factor Scheme for Point Source Configurations," *Int. J. Heat Mass Transfer*, Vol. 17, 1975, pp. 267-272.

10. Morrison, F. A., Jr., and Reed, L.D., "Low Knudsen Number Heat Transfer From Two Spheres in Contact," ASME Journal of Heat Transfer, Vol. 96, 1974, pp. 478-482.

11. Smythe, W. R., *Static and Dynamic Electricity*, 3rd Edition, McGraw-Hill, New York, 1968.

12. Smythe, W. R., "The Capacitance of a Circular Annulus," *American Journal of Physics*, Vol. 22, Dec. 1951, pp. 1499-1501.

13. Smythe, W. R., "Charged Right Circular Cylinder," *Journal of Applied Physics*, Vol. 27, No. 8, 1956, pp. 917-920.

14. Smythe, W. R., "Charged Right Circular Cylinder," *Journal of Applied Physics*, Vol. 33, No. 10, 1962, pp. 2966-2967.

15. Schneider, G. E., "Thermal Resistance Due to Arbitrary Contacts On a Half-Space," *Progress In Astronautics and Aeronautics*, Vol. 65, 1979, Editor, Raymond Viskanta, pp. 103-119.

16. Yovanovich, "New Nusselt and Sherwood Numbers for Arbitrary Isopotential Geometries at Zero Peclet and Rayleigh Numbers," AIAA Paper No. 87-1643, AIAA 22nd Thermophysics Conference, June 8-10, 1987, Honolulu, Hawaii.

17. Yovanovich, M. M. and K. A. Martin, "Some Basic Three-Dimensional Influence Coefficients for the Surface Element Method," AIAA Paper, AIAA 15th Thermophysics Conference, July 14-16, 1980, Snowmass, Colorado.

18. Yovanovich, M. M.,"Thermal Constriction Resistance of Contacts on A Half-Space: Integral Formulation," AIAA Paper 75-708, AIAA 10th Thermophysics Conference, May 27-29,1975, Denver, Colo..

19. Abramowitz, M. and Stegun, I., *Handbook of Mathematical Functions*, Dover Publications, Inc., New York, 1965.

20. Wolfram, S.,*Mathematica, A System for Doing Mathematics by Computer*, Second Edition, Addison-Wesley Publishing Company, Inc., Redwood City, Ca., 1991